

Design for Control of a Soft Bidirectional Bending Actuator

R. Adam Bilodeau^{*1,2}, Michelle C. Yuen^{*1,2}, Jennifer C. Case^{1,2}, Trevor L. Buckner¹,
Rebecca Kramer-Bottiglio^{1,2}

Abstract—In this paper, we present sensor-controlled antagonistic pneumatic actuators (SCAPAs) that integrate proven soft robotic actuators and sensors into a simplified, controllable design. The antagonistic actuators together compose a bidirectional bending actuator with embedded capacitive strain sensors. By designing the SCAPAs from the ground-up for closed-loop control, we are able to minimize both the number of constituent components and the types of materials used, and further streamline the manufacturing processes. These improvements are embodied in the multipurpose use of a single conductive fabric sheet for both actuation and sensing, integrated into an otherwise all-silicone device. Such reduced material complexity allows us to use simple finite element analysis (FEA) models to predict the performance of a given design. We compare various designs to maximize sensor effectiveness using FEA and experimentally verify the suitability of select designs for state reconstruction. After converging on our final design, we demonstrate that this design evaluation process enables the use of simple control strategies to achieve closed-loop control.

Keywords: soft material robotics, hydraulic/pneumatic actuators, sensor-based control

I. INTRODUCTION

Elastomer-based pneumatic actuators have been demonstrated as highly adaptable functional systems [1]. Initial work presenting inflatable “pneu-nets” in an elastomeric body demonstrated that the silicone structures could grip objects or slowly walk when given simple, open-loop commands [2], [3]. Since then, they have seen significant forward progress in their fabrication, adaptability, and control [4]. However, this forward progress has come coupled with both a rise in the manufacturing complexity of casting the pneumatic chambers [5], [6], and in the design complexity as additional sensory systems are embedded [4], [7]–[9]. It has also increased the need for on-demand high-pressures and vacuums [10]–[12] and their corresponding, often bulky, equipment. This trend of increased complexity will likely only rise as researchers strive to derive additional functionality, logic, or adaptability out of otherwise inert soft materials.

One of the challenges of soft robotic systems is in creating reliable controls [13]. Since inflatable soft technologies experience large deformations during operation, and are constructed with viscoelastic materials, closed-loop control is not a trivial task [14]. Though pneumatic actuators were

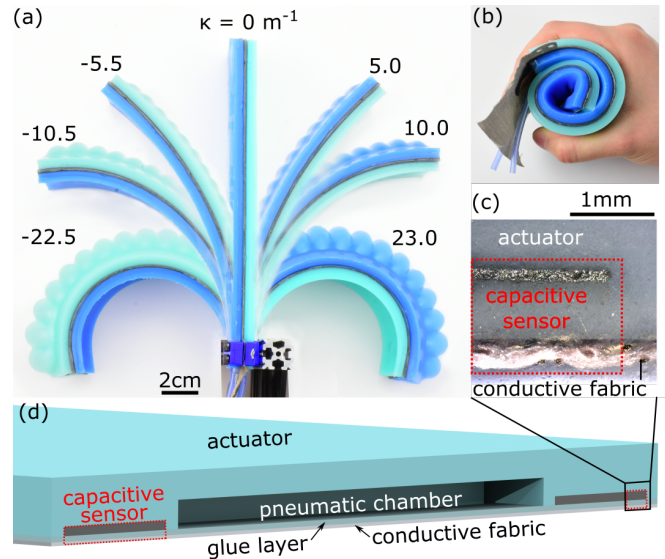


Fig. 1. Sensor-controlled antagonistic pneumatic actuator (SCAPA). (a) Overhead view of a SCAPA sweeping across its full range of achievable curvatures, κ . (b) Due to its fully soft construction, the SCAPA can be rolled up, compressed, and still return to full functionality. (c) Optical microscope image of the interface between the actuator, embedded sensor, and conductive fabric. (d) A cross-section schematic of a SCAPA, including an indicator for the location of the optical image in (c).

demonstrated early on, development of soft sensors capable of matching the physical response of these systems lagged behind. As such, much of the state-of-the-art in soft robotic controls has focused on predictive models and feed-forward controls [15]–[19] or on actuator (pressure) feedback rather than true state reconstruction and closed-loop control via sensors [20], [21]. Recently, there has been an increase in the use of finite element analysis (FEA) to better understand and predict the response of a soft system [5], [22]–[24], but due to material non-linearity and large system deformation, these FEA models are complex and difficult to implement. Forays into sensor-enabled closed-loop control have used commercially available flexible sensors to demonstrate state reconstruction and control [25]–[27]. These sensors also provide a strain-limiting layer while providing the state-reconstruction feedback.

Recent advances in silicone-based all-soft sensors are beginning to allow for more advanced demonstrations of closed-loop control in soft actuators. Early soft sensors used conductive liquid metals embedded in elastomer as high-deformation resistive sensors [28], [29]. These have been used both as embedded sensors for state reconstruction and

*RAB and MCY are co-first authors.

¹School of Engineering and Applied Science, Yale University, New Haven, CT, USA

²School of Mechanical Engineering, Purdue University, West Lafayette, IN, USA rbilodea@purdue.edu, yuenm@purdue.edu, rebecca.kramer@yale.edu

as external sensors for closed-loop control [6], [8], [30], [31]. More recently, soft conductive silicone composites have been demonstrated as reliable, repeatable, high-deflection capacitive sensors that can be placed externally on soft joints for 2D and 3D state reconstruction [32]–[36] or as integrated resistive sensors providing both proprioception and tactile feedback in closed-loop controlled pneumatic grippers [37]. As an alternative, stretchable optics have been demonstrated as embedded sensors in pneumatic actuators, providing state reconstruction, curvature control, and tactile feedback [7], [38]. With all this available research into soft sensors and controllable soft systems, we see an opportunity to synthesize simpler robotic constructs without losing functionality or utility.

In this paper, we present sensor-controlled antagonistic pneumatic actuators (SCAPAs, Figure 1) which integrate proven soft robotic actuation and sensing technologies in a simplified design targeting controllability of the system state (*i.e.* design for control). Specifically, we embed silicone-based capacitive strain sensors [39] into pneu-net bending actuators [1], which we then assemble as antagonistic pairs to achieve bi-directional, controllable actuation. Compared to previous work, we make two key improvements to the system: 1) utilizing inextensible conductive fabric as both the strain-limiting layer for the actuators and the ground plane for the capacitive sensors, and 2) utilizing the same silicone material in both the actuators and sensors. These improvements result in fewer constituent components, fewer interfaces between dissimilar materials, and fewer manufacturing steps. This reduction in physical complexity allows us to use a simple FEA model to predict the quality of a given design, which we experimentally verify. We compare various candidate designs using the FEA model and subsequent experimental tests to determine which design can provide strong state reconstruction. Finally, we select a SCAPA design and use it to demonstrate closed-loop curvature control using various basic feedback control strategies.

II. PHYSICAL EMBODIMENT

A SCAPA consists of an antagonistic pair of thin bending pneumatic actuators, each with an embedded capacitive sensor for differential measurement of curvature (Figure 1). At the core of each SCAPA is conductive fabric, which serves dual purposes as both the strain-limiting layer for the actuators and as the grounding electrode for the sensors. The system’s reduced profile allows us to roll a SCAPA into a compact cylinder without damaging any of the constituent components (Figure 1(b)). Previous work used conductive fabric as both the strain-limiting layer of a one-sided pneumatic actuator and an electrode for capacitive contact detection [40]. Here, we expand on their work by using the fabric in a state feedback sensor for closed-loop control, rather than object detection.

The sensors are constructed as a parallel-plate capacitor using an expanded graphite silicone composite for the active conductive layer and unmodified silicone elastomer for the dielectric layer. As the sensor geometry changes

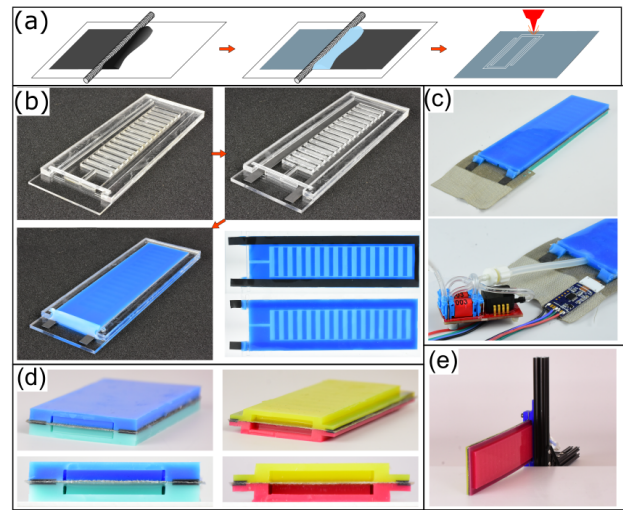


Fig. 2. (a-c) Manufacturing the SCAPA. (a) The capacitive sensors were first fabricated in large films and then laser cut into the desired patterns. (b) The casting process created the pneu-net actuators while simultaneously embedding a sensor in the actuator body. (c) Conductive fabric was glued between two actuators to create the antagonistic bending system and the electronics controlling actuation and measure the sensors were attached to the SCAPA. (d) Photos showing two of the designs explored. The actuator body, sensors, and conductive fabric are clearly visible in the cross-sectional images. (e) For all experiments performed, each SCAPA was fixed vertically such that the tip would sweep horizontally. A camera was situated above the SCAPA to record truth data on its curvature.

due to applied strain or pressure, the capacitance changes measurably. White, *et al.* previously conducted a study of the materials and manufacturing of these strain sensors, as well as their response to many cycles of strain [39]. We made the sensors out of the same elastomer as was used in the actuator body, resulting in a nearly invisible, fully bonded interface between the sensor and actuator (Figure 1(c)). This material continuity reduces risk of delamination failure that can occur at interfaces between dissimilar materials. We also leverage the single material construction to simplify analysis of strain fields in the device’s silicone walls.

To bend a SCAPA, one of the actuators is inflated while the other is vented to atmosphere. This bend causes the capacitance of the embedded sensors to change. The actuator inflation is controlled by “pneumatic servos” which serve effectively as 3-port, digital pressure regulators [41]. To read the capacitance change, we use custom signal conditioning boards that charge the sensor for a fixed length of time and record the time it takes to discharge to ground voltage (based on [39] with modified software). The entire system is controlled using an Arduino Mega communicating with the pneumatic servos and the sensor signal conditioning boards via I2C protocol.

A. Fabrication

The SCAPAs were manufactured in three phases: 1) sensor fabrication, 2) actuator casting, and 3) assembly (Figure 2(a-c)). As stated previously, the conductive fabric acted as a shared ground layer for both capacitive sensors. To make the rest of the sensor, we cast the remaining two layers in

a sheet by rod-coating first the silicone-graphite composite (DragonSkin 10 Slow, Smooth-On; Expandable graphite, Sigma-Aldrich) for the active electrode layer [39], followed by the pure silicone for the dielectric layer (DragonSkin 10 Slow) (Figure 2(a)). Upon curing, we used a laser to cut out two U shapes that fit along the outside edges of the actuators. We cleaned the cut shapes with ethanol and laid them in the bottom of the actuator molds. The molds were fabricated from laser-cut acrylic sheets (Figure 2(b)). We poured silicone into the molds (DragonSkin10 Slow; SilcPig silicone dye, Smooth-On), degassed the cast material in a vacuum chamber, and clamped a lid on top to ensure uniform thickness across all actuators. After the actuators cured, we glued one to each side of inextensible conductive fabric (Technicot, LessEMF) using additional uncured silicone, completing both the actuators and the sensors. The tubing for the actuators was inserted and epoxied to the actuator body (Sil-Poxy, Smooth-On), and connected to the pneumatic servos (Figure 2(c)). The capacitance signal conditioning boards were sewn directly to the grounding fabric to improve the electrical contact between the two. Flexible copper-clad polyimide strip electrodes extending from the signal conditioning boards were sandwiched against the active silicone sensor layer by two polystyrene plates that were also sewn to the fabric. These strip electrodes allowed for a larger contact area between the interfacing surfaces, giving the signal conditioning board a strong electrical connection to the active layer.

III. DESIGN

In order to properly characterize and study a symmetric actuator sensor pair, we defined a simple, perspective-based nomenclature to differentiate the sensors and the curvature of the SCAPA. From the top-down perspective shown in Figure 1(a), when the right-side actuator is inflated, the SCAPA body will bend to the left, which we define as a negative curvature. Conversely, when the left actuator is inflated, the SCAPA body bends to the right, which we define as a positive curvature. The sensors located in the left and right actuators are referred to as the left and right sensors, respectively.

In theory, when the curvature is positive, the capacitance of the left sensor should increase due to stretching and Poisson thinning of the dielectric layer. Similarly, the right sensor should increase in capacitance as the sensor length is compressed. By convolving the two sensor signals it should be possible to determine the curvature of the SCAPA for state feedback to the controller [31].

In practice, with a highly deformable sensor embedded in the actuator, we must consider how the sensor response is coupled to all deformations in the soft body, from those we want to measure (curvature proprioception) and those we do not want to measure (inflation expansion). To address this coupled response, we performed a design study of the cross-sectional geometry to develop designs in which the sensors would be minimally affected by actuator pressure. This design study consisted of two parts: 1) FEA modeling

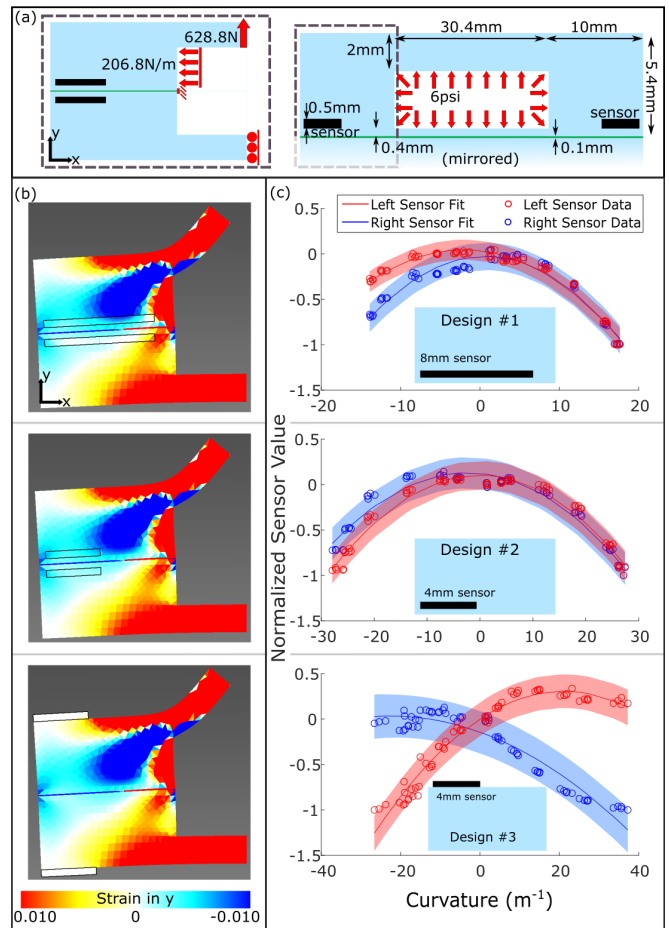


Fig. 3. Design study to determine the effects of sensor width and placement on the quality of the sensor output. (a) Schematic of the loading conditions for the FEA (left) and cross-section geometry (right), with only the boxed section being modeled. (b) Sketches of the initial modeled geometry and the FEA results. Design 1 shows the base case for the system. Design 2 reduces the width of the sensor and Design 3 moves sensor to the top of the actuator. (c) Experimental verification plots showing the sensor responses to curvature. The circles indicate experimental data and the line is a quadratic fit with the shaded region being a 95% confidence bound about the regression.

to predict deformation fields in the actuator cross-section due to inflation expansion, and 2) empirical verification of the design's effect on sensor response.

A. FEA modeling of cross-section

A series of FEA simulations were run in SolidWorks to assess the deformation in the sensor region due to inflation (Figure 3). The analyses were set up using a 2D cross-section of the SCAPA, with reduced geometry to encourage faster solution times. Expecting large deformations in the wall, the simulations were run using a nonlinear solver. Our model includes three assumptions:

- 1) A fixed fabric layer that is completely inextensible, perfectly flexible, and perfectly bonded to the silicone. We are confident with this assumption due to the orders-of-magnitude difference in tensile elasticity between the silicone and fibers in the fabric, and because we chose

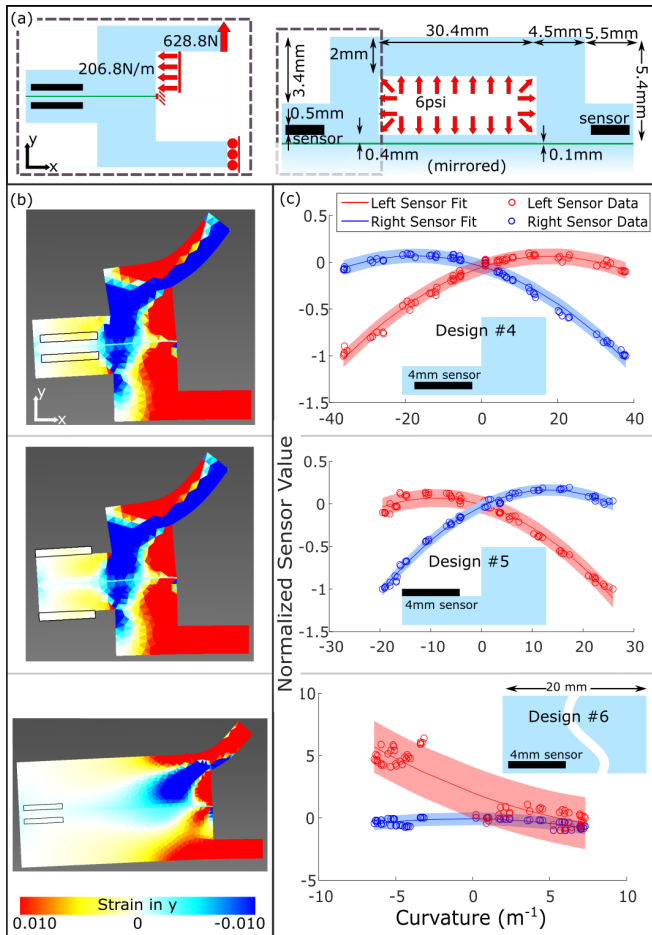


Fig. 4. Design exploration of various geometries that should limit the effect of actuator inflation on sensor response. (a) Schematic of the the loading conditions for the FEA (left) and the cross-section geometry (right), with only the boxed section being modeled. (b) Sketches of the initial modeled geometry and the FEA results. Design 4 and 5 introduce a notch along the outer edge of the actuator with the sensor embedded near the fabric layer and on top of the notch respectively. Design 6 increases the distance between the sensor and the pneu-nets by increasing the width of the actuator wall. (c) Experimental verification plots showing the sensor responses to curvature. Design 6 began to twist while actuating resulting in unpredictable sensor responses. The circles indicate experimental data and the line is a quadratic fit with the shaded region being a 95% confidence bound about the regression.

a fabric with an open weave that allowed the pre-cured silicone to fully permeate between all the fibers.

- 2) Uniform material throughout the elastomer, since both the sensor and the actuator are silicone, the active composite layer is very thin, and there is little conductive filler in the composite itself.
- 3) Linear elastic behavior of the silicone, where $E = 0.12$ MPa, obtained via a linear extension test on dogbone shaped silicone samples using an Instron 3345 materials testing system, with samples tested to 50% strain at 100% strain per minute.

Previous work showing detailed 3D analysis of an inflating elastic chamber indicate that the thick outer walls experience stresses that are 2-3 orders of magnitude less than the thin, expanding ‘roof’ of the chamber [22]. Since our soft sensors

are placed along the outer wall of the device, we considered only this section as our area of interest, and simplify our model accordingly. This simplification is further supported by inspecting additional modeling work that has recently been performed [5], [23]. Instead of applying pressure to a geometric reconstruction of the whole cross section, we applied an upward force equivalent to the pressure lifting the pneumatic pocket, acting along a moment arm. This accounted for both a lifting motion and bending moment experienced at the juncture between the pneumatic pocket and the actuator wall (Figure 3(a)). We then applied the remaining internal pressure directly to the wall’s edge. Due to symmetry, it was only necessary to analyze one side of the structure.

In this analysis, we were primarily interested in sensor strain in the y-direction (normal to the fabric), as defined by the axes in Figure 3(a). Since one half of the parallel-plate capacitor is a wide fabric sheet, sensor displacement in the x-direction should not affect the sensor output. However, y-strain will have a significant impact on the sensor, as it reflects changes in the distance between the electrodes, while discounting bulk motion of the entire system in the y-direction. Any y-strain in and under the sensor induces a sensory response that is not reflective of the SCAPA’s bending motion. By marking out the area of the sensor in our FEA model, and plotting the strain in the y-direction, we clearly see the effects of actuator inflation on compression and tension in the sensor (Figure 3(b)).

B. Sensor Characterization & Model Verification

To verify the FEA modeling, we initially modeled three designs with different sensor sizes (8mm or 4mm wide) and locations (embedded or on top of actuator) and then built these designs to experimentally evaluate their viability for curvature state reconstruction (Designs 1, 2 and 3, shown in Figure 3(b-c)). Using the experimental setup shown in Figure 2(e), we mounted the SCAPAs onto a stand such that both actuators were perpendicular to the benchtop. We sewed a thin strip of Teflon to the tip of the actuator to minimize friction during motion. A webcam was mounted overhead to record the curvature truth data of each SCAPA during actuation. In each experiment, we actuated both actuators individually through a range of inflation pressures between 6-11 psi (at 1 psi increments and five repetitions at each pressure), in a randomized order. This range of pressures correspond to the range of curvatures shown in Figure 1. Once inflated to the desired pressure, we allowed the actuator to settle into a steady state for 5 s. We then sampled and recorded the sensors 100 times over a period of 10 s and averaged the data to obtain a representative sensor reading. Finally, we took a photo of the actuator from which we measured the curvature of the actuator (truth data) using a three-point fitting algorithm that assumes constant curvature in the system.

We plotted the sensor values against the curvature to evaluate the design’s performance (Figure 3(c)). We first normalized the sensor data to the data range between 0

curvature (x_0) and the minimum measured sensor value (x_{min}): $x_{norm} = (x - x_0)/(x_0 - x_{min})$. In an ideal bending beam, negative curvatures would correspond to the right sensor's capacitance increasing and the left sensor's capacitance decreasing, with the converse expected when bending to the right. Instead, we observed that both sensors have a parabolic response. In Designs 1 and 2, this response is centered near a curvature of 0 m^{-1} , while the response in Design 3 shows a significant offset. Because of this, the positive and negative curvatures for Designs 1 and 2 cannot be well-distinguished, even when convolving the two sensor signals. We hypothesize that this is due to the sensor response being coupled with inflation pressures. As suggested by the FEA models for these two designs, there is a field of y -strain (marked in blue) cutting through the location of the sensors. Design 3's asymmetric response corroborates the conclusions from the FEA, which suggests that only a portion of the area under the sensor is undergoing strain, and so the sensor is only marginally affected by actuator inflation. This initial design study showed us that our FEA model is able to predict the impact of sensor placement in a cross-section, even with our embedded modeling assumptions.

C. Design Exploration

Having experimentally verified our FEA model, we used it to qualitatively examine multiple cross-section designs without the need for building physical prototypes. After testing many designs that varied in geometric parameters, we removed those that performed poorly in the FEA models and converged on three designs (Designs 4, 5, and 6, shown in Figure 4(b)). These designs minimized the impact of the actuation pressure on the sensor, and we fabricated each design to confirm the results of the FEA. Designs 4 and 5 introduce a stress-relieving notch in the actuator wall above the sensor; Design 6 widens the wall of the actuator and moves the sensors further away from the pneu-nets.

Our results show that the notched designs isolated the sensors from a significant portion of the actuator inflation deformation. The sensors' responses in Designs 4 and 5 show unique pairings of left and right sensor values across the entire range of curvatures tested. Compared to Design 3, the confidence bounds on Design 4 and 5 are greatly reduced, indicating a stronger and more repeatable response to curvature change. Additionally, we observed that the sensor values rise above 0, indicating that the sensors' capacitances increase as expected, albeit slightly, when it is on the outside of the curve.

The results of the experimental characterization of Design 6 indicate a breakdown in our simplified FEA model. The increased wall width changed the deformation dynamics of the actuator. Rather than simply bending, the SCAPA twisted and/or curled into a bowl-like shape, which resulted in highly unusual, asymmetric sensory response (Figure 4). This sort of dynamic 3D response was not accounted for in our simplified 2D FEA, indicating a model limitation.

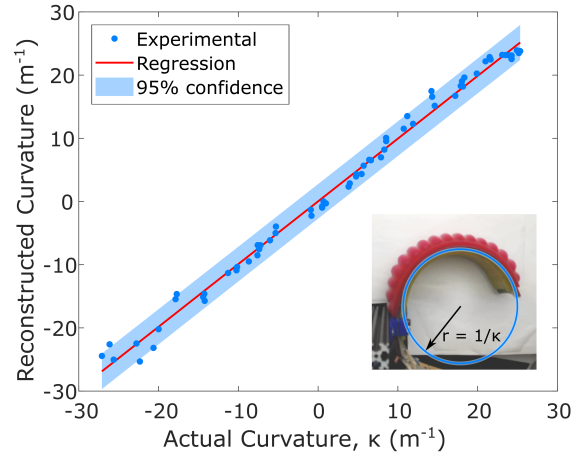


Fig. 5. Sensor calibration results for Design 4 (see Figure 4) comparing the actual curvature to state reconstructed curvature. The shaded region represents the 95% confidence interval. The inset shows an inflated SCAPA with a fitted circle used to measure the actual curvature. r is the radius of the circle and κ is the curvature.

IV. CLOSED LOOP CONTROL

A. SCAPA Design Selection

We chose to use Design 4 to demonstrate closed loop control. This particular design (demonstrated in Figure 2(d)) met all of the goals we sought to achieve for improved state estimation: simplified manufacturing with embedded sensing cast into the actuator in a single-step, a sensory response to actuator strain in which both actuators produced distinct responses to the actuator's shape change, and low variation in the sensory response with respect to curvature. After choosing this design, we then remounted the system in our testing setup, we and collected a new set of calibration data using a higher refinement in pressure steps (incrementing by 0.5 psi) to get a better resolution in curvatures.

B. Empirical Model

Once the sensor data was correlated with the measured curvature of the system, a generalized least squares regression was used to determine the coefficients for the following equation:

$$\kappa = a_0 + a_1 S_1 + a_2 S_2$$

where κ is the curvature of the SCAPA, S_i are the raw sensor output values from the sensor boards, and the constants a_i are the coefficients of the fit. Using the regression model, we reconstructed the curvature for each set of sensor values gathered during calibration, and plotted it against the measured curvature values (see Figure 5). The fit has a 95% confidence interval of 5.549 m^{-1} or 10.58% of the full scale.

C. Controllers

We tested the system response of our SCAPA using three different controllers (Table I). These controllers are composed of two different control loops (a logic loop and a proportional-logic loop, diagrammed in Figure 6) with two different internal logic controllers (whose state machines are

TABLE I

NAMING CONVENTION FOR THE THREE CONTROLLERS IMPLEMENTING THE CONTROL LOOPS IN FIGURE 6 AND STATE MACHINES IN FIGURE 7.

| Controller Name | Control Loop | State Machine |
|----------------------------------|----------------------|---------------|
| Simultaneous | Logic | Dynamic |
| Fixed Rate Quasi-Static (FRQS) | Logic | Quasi-Static |
| Varying Rate Quasi-Static (VRQS) | Logic + Proportional | Quasi-Static |

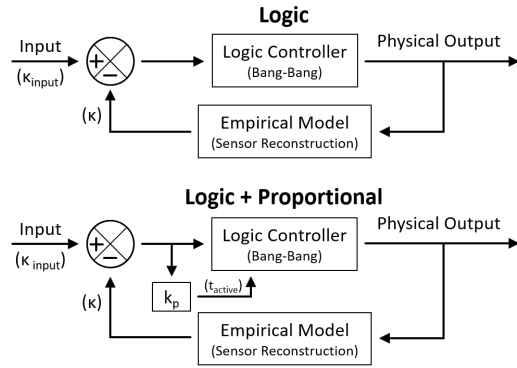


Fig. 6. Control loops used to follow the input signal.

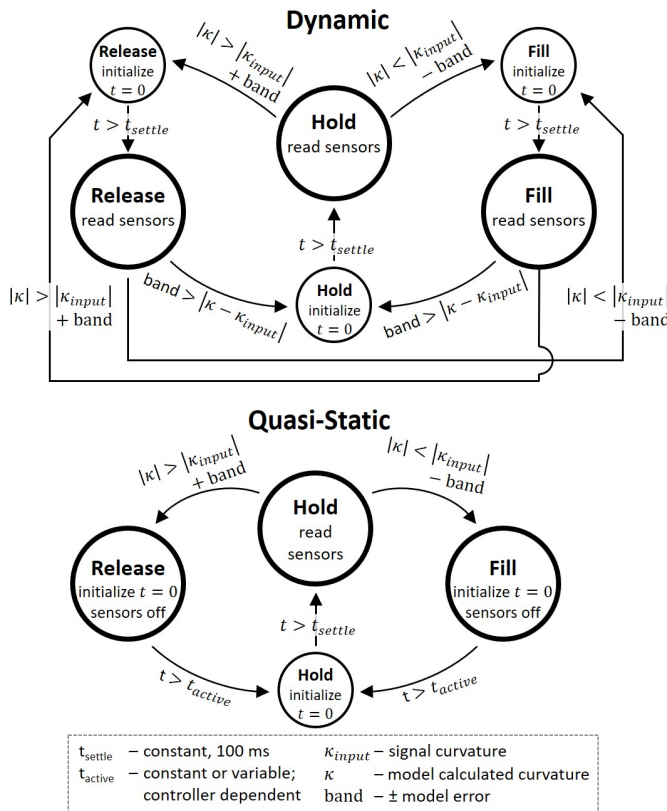


Fig. 7. State machines used in the logic controllers.

sketched in Figure 7). We used a target curvature (κ_{input}) as the input signal for all three controllers. This signal could be either positive or negative, and all three logical controllers had a built-in filter to switch between which of the two actuators was active, based on the sign of the desired curve.

The physical design of the SCAPA instilled some common requirements for each controller. First, since the inactive actuator was compressed during actuation, it was always held in the ‘deflate’ state to ensure that its internal pressure was equal to atmosphere. Second, the capacitive sensors are sensitive to the activation of the solenoids in the pneumatic servos [41]. To compensate, we added intermediary ‘settling time’ states with a fixed delay ($t_{settle} = 100$ ms) in which sensor-reading was locked out (all smaller circles in Figure 7). Finally, the hold response of all three controllers would trigger if the sensory response was within a band around the signal curvature, derived from the model error (see Figure 5).

As outlined in Table I, we named each controller based on the operation goal. The simultaneous controller, the most basic controller we could implement, is a logic controller that increases, holds, or releases pressure in the pneumatic actuator, while sampling the sensors simultaneously. The quasi-static logic state machine removes the dynamic response of the physical system from the sensor data by locking out the sensor reading when the actuator is inflating or deflating. The inflation or deflation time was either fixed (fixed rate quasi-static controller, FRQS) or could vary proportionally to the curvature error (varying rate quasi-static controller, VRQS). The FRQS controller used only fixed values for all of the timings, coded directly into the logic controller. It operated on a 250 ms cycle frequency, actuating for 50 ms, settling for 150 ms, and then reading the sensors 10 times during the last 100 ms (and averaging the data). In contrast, the VRQS controller used proportional control to determine the timing that the actuator should be allowed to inflate/deflate (between 0-450 ms). Since the proportional timings allowed for much larger inflate/deflate times during large jumps in the input signal, we were able to allow the system to settle for longer (350 ms) without slowing down the overall performance, and thus improve the sensor data retrieved and therefore the accuracy of the controller.

D. System Response

The responses of the three controllers are shown in Figure 8. The input signal is shown as a solid black line, with the mean system response shown as a solid blue line and 95% confidence error bound shaded. For each controller, we also calculated the mean error in curvature of the experimental response from the signal (the average absolute difference between the signal curvature and the SCAPA’s curvature at any given moment in time) in order to quantitatively judge the three different controllers.

As is evident in Figure 8, the simultaneous controller performed poorly, with the system having an average curvature error of 17.6 m^{-1} . The immediate, continuous feedback caused the controller to whip the actuator back and forth

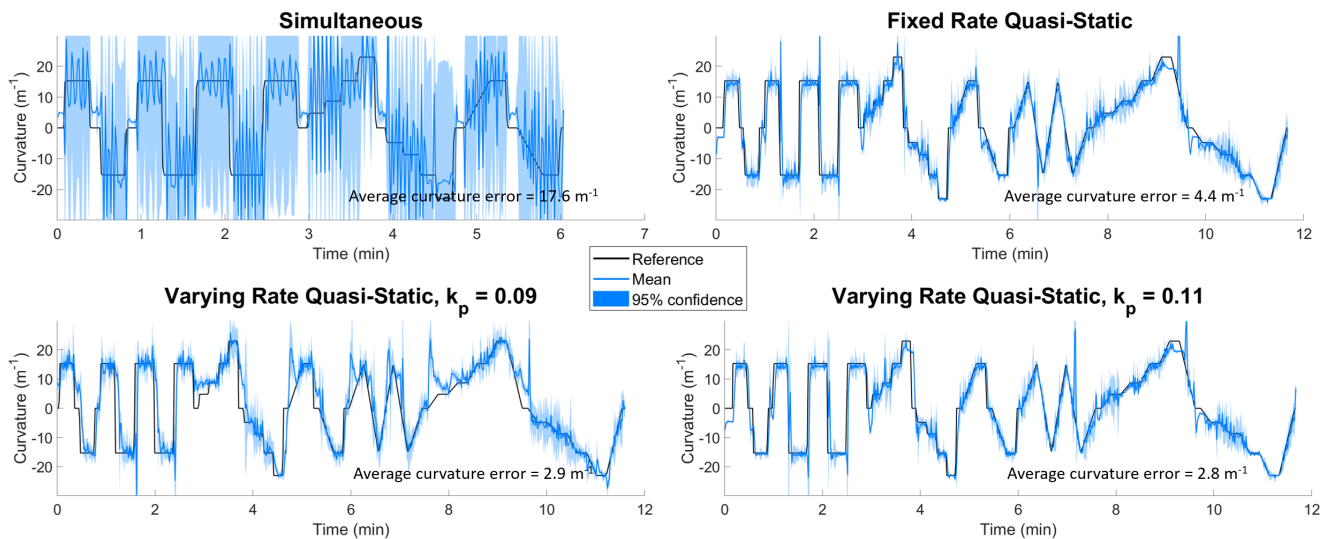


Fig. 8. Closed-loop curvature control using the Simultaneous, Fixed Rate Quasi-Static, and Varying Rate Quasi-Static controllers, with two different proportional gains in the VRQS controller. Each plot shows the reference signal (black) and the reconstructed curvature (blue - both mean and 95% confidence bounds), and indicates the mean deviation (error) of the system response from the desired curvature for the whole test.

so wildly that we discontinued the test before completion to prevent damage to the actuator. We hypothesize that the (potentially internal oscillatory) dynamic response of the physically inflating system was coupled into the sensor response in a way that was unpredicted in our quasi-static empirical model, causing the measured curvature to vary.

Switching to the FRQS controller, the SCAPA's performance improved, with an average curvature error of only 4.4 m^{-1} . This immediate improvement further reinforced our conclusion about the simultaneous controller: that the internal dynamics of the physical silicone, combined with the sensitivity of our sensors, resulted in sensor responses that gave inaccurate feedback to the logic control loop. In order to improve the error further, we allowed the fill time to vary with a proportional controller. We tested two different gains (0.09 and 0.11) and the average error reduced to 2.9 m^{-1} and 2.8 m^{-1} , respectively. This exercise demonstrates that soft-bodied control is achievable using a just simple proportional control loop.

V. CONCLUSION AND FUTURE WORK

In this paper, we presented sensor-controlled antagonistic pneumatic actuators (SCAPAs), designed for simplified fabrication and control. Towards streamlined and efficient fabrication, we utilized conductive fabric to serve as both the inextensible layer for the actuators enabling bending, and as the ground layer of the embedded capacitive sensors. In order to achieve curvature control, we designed the SCAPAs so that the embedded sensors would respond to curvature, rather than actuator inflation. We used FEA modeling and experimental characterization of the sensor response to curvature to evaluate various SCAPA geometries and determine an appropriate design. After selecting an appropriate design, we demonstrated that the chosen SCAPA design could be controlled with a simple quasi-static control strategy with

only minimal error. With both functional antagonistic actuators and feedback sensors, the SCAPA we presented is a fully autonomous, soft pneumatic robot.

Future efforts will explore the dynamic behavior of the SCAPAs and expand from a single SCAPA to multiple units connected in series to form a fully controllable soft continuum manipulator. Future work will also focus on exploration of the FEA, quantitatively comparing run-time and model complexity with the physical response. By changing the assumptions, material properties, modeled regions and including out-of-plane stresses, which can result in additional unexpected warping and buckling, we will be able to optimize the model for both speed and result quality. Additionally, a quantitative comparison of presented control strategies and additional controllers (for example, PID), each with optimized timings and gains, should be studied through automated empirical testing. Finally, coupled sensor responses could be used to determine when an external force is acting on the SCAPA.

VI. ACKNOWLEDGMENTS

The authors would like to thank Dylan S. Shah for assisting with the operation of the pneumatic servos, and Dr. Joran W. Booth for his assistance in assembling the controllers. This work was supported by the US Air Force Office of Scientific Research under award number FA9550-16-1-0267, by which RAB was funded. MCY is supported by the National Science Foundation Graduate Research Fellowship (Grant DGE-1333468). JCC is supported by the National Aeronautics and Space Administration Space Technology Research Fellowship program (Grant NNX15AQ75H).

REFERENCES

- [1] F. Ilievski, A. D. Mazzeo, R. F. Shepherd, X. Chen, and G. M. Whitesides, "Soft Robotics for Chemists," *Angewandte Chemie International Edition*, vol. 50, pp. 1890–1895, Feb. 2011.
- [2] A. A. Stokes, R. F. Shepherd, S. A. Morin, F. Ilievski, and G. M. Whitesides, "A Hybrid Combining Hard and Soft Robots," *Soft Robotics*, vol. 1, pp. 70–74, July 2013.

- [3] R. F. Shepherd, F. Ilievski, W. Choi, S. A. Morin, A. A. Stokes, A. D. Mazzeo, X. Chen, M. Wang, and G. M. Whitesides, "Multigait soft robot," *Proceedings of the National Academy of Sciences*, vol. 108, pp. 20400–20403, Dec. 2011.
- [4] P. Polygerinos, N. Correll, S. A. Morin, B. Mosadegh, C. D. Onal, K. Petersen, M. Cianchetti, M. T. Tolley, and R. F. Shepherd, "Soft Robotics: Review of Fluid-Driven Intrinsically Soft Devices; Manufacturing, Sensing, Control, and Applications in Human-Robot Interaction," *Advanced Engineering Materials*, vol. 19, p. 1700016, Dec. 2017.
- [5] B. Mosadegh, P. Polygerinos, C. Keplinger, S. Wennstedt, R. F. Shepherd, U. Gupta, J. Shim, K. Bertoldi, C. J. Walsh, and G. M. Whitesides, "Pneumatic Networks for Soft Robotics that Actuate Rapidly," *Advanced Functional Materials*, vol. 24, pp. 2163–2170, Apr. 2014.
- [6] R. A. Bilodeau, E. L. White, and R. K. Kramer, "Monolithic fabrication of sensors and actuators in a soft robotic gripper," in *2015 IEEE/RSJ International Conference on Intelligent Robots and Systems (IROS)*, pp. 2324–2329, Sept. 2015.
- [7] H. Zhao, K. O'Brien, S. Li, and R. F. Shepherd, "Optoelectronically innervated soft prosthetic hand via stretchable optical waveguides," *Science Robotics*, vol. 1, p. 10, Dec. 2016.
- [8] N. Farrow and N. Correll, "A soft pneumatic actuator that can sense grasp and touch," in *2015 IEEE/RSJ International Conference on Intelligent Robots and Systems (IROS)*, pp. 2317–2323, Sept. 2015.
- [9] C. M. Best, J. P. Wilson, and M. D. Killpack, "Control of a pneumatically actuated, fully inflatable, fabric-based, humanoid robot," in *2015 IEEE-RAS 15th International Conference on Humanoid Robots (Humanoids)*, pp. 1133–1140, Nov. 2015.
- [10] M. T. Tolley, R. F. Shepherd, B. Mosadegh, K. C. Galloway, M. Wehner, M. Karpelson, R. J. Wood, and G. M. Whitesides, "A Resilient, Untethered Soft Robot," *Soft Robotics*, vol. 1, pp. 213–223, Sept. 2014.
- [11] D. Yang, B. Mosadegh, A. Ainla, B. Lee, F. Khashai, Z. Suo, K. Bertoldi, and G. M. Whitesides, "Buckling of Elastomeric Beams Enables Actuation of Soft Machines," *Advanced Materials*, vol. 27, pp. 6323–6327, Nov. 2015.
- [12] M. A. Robertson and J. Paik, "New soft robots really suck: Vacuum-powered systems empower diverse capabilities," *Science Robotics*, vol. 2, p. eaan6357, Aug. 2017.
- [13] B. Trimmer, "Soft Robot Control Systems: A New Grand Challenge?," *Soft Robotics*, vol. 1, pp. 231–232, Dec. 2014.
- [14] D. Rus and M. T. Tolley, "Design, fabrication and control of soft robots," *Nature*, vol. 521, pp. 467–475, May 2015.
- [15] E. H. Skorina, M. Luo, S. Ozel, F. Chen, W. Tao, and C. D. Onal, "Feedforward augmented sliding mode motion control of antagonistic soft pneumatic actuators," in *2015 IEEE International Conference on Robotics and Automation (ICRA)*, pp. 2544–2549, May 2015.
- [16] C. M. Best, M. T. Gillespie, P. Hyatt, M. D. Killpack, L. Rupert, and V. Sherrod, "Model predictive control for pneumatically actuated soft robots," *Robotics and Automation Magazine. IEEE*, 2015.
- [17] M. T. Gillespie, C. M. Best, and M. D. Killpack, "Simultaneous position and stiffness control for an inflatable soft robot," in *2016 IEEE International Conference on Robotics and Automation (ICRA)*, pp. 1095–1101, May 2016.
- [18] E. H. Skorina, W. Tao, F. Chen, M. Luo, and C. D. Onal, "Motion control of a soft-actuated modular manipulator," in *2016 IEEE International Conference on Robotics and Automation (ICRA)*, pp. 4997–5002, May 2016.
- [19] S. I. Rich, R. J. Wood, and C. Majidi, "Untethered soft robotics," *Nature Electronics*, vol. 1, pp. 102–112, Feb. 2018.
- [20] A. D. Marchese, K. Komerowski, C. D. Onal, and D. Rus, "Design and control of a soft and continuously deformable 2d robotic manipulation system," in *2014 IEEE International Conference on Robotics and Automation (ICRA)*, pp. 2189–2196, May 2014.
- [21] P. Polygerinos, Z. Wang, K. C. Galloway, R. J. Wood, and C. J. Walsh, "Soft robotic glove for combined assistance and at-home rehabilitation," *Robotics and Autonomous Systems*, vol. 73, pp. 135–143, Nov. 2015.
- [22] R. V. Martinez, J. L. Branch, C. R. Fish, L. Jin, R. F. Shepherd, R. M. D. Nunes, Z. Suo, and G. M. Whitesides, "Robotic Tentacles with Three-Dimensional Mobility Based on Flexible Elastomers," *Advanced Materials*, vol. 25, pp. 205–212, Jan. 2013.
- [23] P. Moseley, J. M. Florez, H. A. Sonar, G. Agarwal, W. Curtin, and J. Paik, "Modeling, Design, and Development of Soft Pneumatic Actuators with Finite Element Method: Modeling, Design, and Development of SPAs with FEM," *Advanced Engineering Materials*, vol. 18, pp. 978–988, June 2016.
- [24] G. Agarwal, M. A. Robertson, H. Sonar, and J. Paik, "Design and Computational Modeling of a Modular, Compliant Robotic Assembly for Human Lumbar Unit and Spinal Cord Assistance," *Scientific Reports*, vol. 7, Dec. 2017.
- [25] B. S. Homberg, R. K. Katzschmann, M. R. Dogar, and D. Rus, "Haptic identification of objects using a modular soft robotic gripper," in *2015 IEEE/RSJ International Conference on Intelligent Robots and Systems (IROS)*, pp. 1698–1705, Sept. 2015.
- [26] S. Ozel, E. H. Skorina, M. Luo, W. Tao, F. Chen, Y. Pan, and C. D. Onal, "A composite soft bending actuation module with integrated curvature sensing," in *2016 IEEE International Conference on Robotics and Automation (ICRA)*, pp. 4963–4968, May 2016.
- [27] K. Elgeneidy, N. Lohse, and M. Jackson, "Bending angle prediction and control of soft pneumatic actuators with embedded flex sensors A data-driven approach," *Mechatronics*, Oct. 2017.
- [28] H.-J. Kim, C. Son, and B. Ziaie, "A multi-axial stretchable interconnect using liquid-alloy-filled elastomeric microchannels," *Applied Physics Letters*, vol. 92, p. 011904, Jan. 2008.
- [29] R. K. Kramer, C. Majidi, R. Sahai, and R. J. Wood, "Soft curvature sensors for joint angle proprioception," in *2011 IEEE/RSJ International Conference on Intelligent Robots and Systems (IROS)*, pp. 1919–1926, 2011.
- [30] Y. L. Park and R. J. Wood, "Smart pneumatic artificial muscle actuator with embedded microfluidic sensing," in *2013 IEEE SENSORS*, pp. 1–4, Nov. 2013.
- [31] J. C. Case, E. L. White, and R. K. Kramer, "Sensor enabled closed-loop bending control of soft beams," *Smart Materials and Structures*, vol. 25, no. 4, p. 045018, 2016.
- [32] E. L. White, J. C. Case, and R. Kramer-Bottiglio, "A Soft Parallel Kinematic Mechanism," *Soft Robotics*, vol. 5, pp. 36–53, Dec. 2017.
- [33] E. L. White, M. C. Yuen, and R. K. Kramer, "Distributed sensing in capacitive conductive composites," in *2017 IEEE SENSORS*, pp. 1–3, Oct. 2017.
- [34] T. Giffney, E. Bejanin, A. S. Kurian, J. Trivas-Sejdic, and K. Aw, "Highly stretchable printed strain sensors using multi-walled carbon nanotube/silicone rubber composites," *Sensors and Actuators A: Physical*, vol. 259, pp. 44–49, June 2017.
- [35] M. C.-S. Yuen, T. R. Lear, H. Tonoyan, M. Telleria, and R. Kramer-Bottiglio, "Toward Closed-Loop Control of Pneumatic Grippers During Pack-and-Deploy Operations," *IEEE Robotics and Automation Letters*, vol. 3, pp. 1402–1409, July 2018.
- [36] J. C. Case, J. Booth, D. S. Shah, M. C. Yuen, and R. Kramer-Bottiglio, "State and stiffness estimation using robotic fabrics," in *2018 IEEE International Conference on Soft Robotics (RoboSoft)*, pp. 522–527, IEEE, Apr. 2018.
- [37] Y. Yang and Y. Chen, "Innovative Design of Embedded Pressure and Position Sensors for Soft Actuators," *IEEE Robotics and Automation Letters*, vol. 3, pp. 656–663, Apr. 2018.
- [38] H. Zhao, R. Huang, and R. F. Shepherd, "Curvature control of soft orthotics via low cost solid-state optics," in *2016 IEEE International Conference on Robotics and Automation (ICRA)*, pp. 4008–4013, May 2016.
- [39] E. L. White, M. C. Yuen, J. C. Case, and R. K. Kramer, "Low-Cost, Facile, and Scalable Manufacturing of Capacitive Sensors for Soft Systems," *Advanced Materials Technologies*, vol. 2, p. 1700072, Sept. 2017.
- [40] N. Farrow, L. McIntire, and N. Correll, "Functionalized textiles for interactive soft robotics," in *2017 IEEE International Conference on Robotics and Automation (ICRA)*, pp. 5525–5531, May 2017.
- [41] J. W. Booth, J. C. Case, E. L. White, D. S. Shah, and R. Kramer-Bottiglio, "An Addressable Pneumatic Regulator for Distributed Control of Soft Robots," in *2018 IEEE International Conference on Soft Robotics (RoboSoft)*, pp. 25–30, IEEE, Apr. 2018.